Wide-Band Equal-Ripple Filters in Nonuniform Transmission Lines

Da-Chiang Chang and Ching-Wen Hsue, *Senior Member, IEEE*

***Abstract*—In this paper, a novel method to realize equal-ripple filters over microwave frequencies is presented. All networks are implemented by using cascade serial and shunt transmission-line sections having the same electrical length. The transfer functions of such networks are formulated in the Z domain. In particular, it can be shown that some shunt components are able to contribute zeros locating on the unit circle if the components are open circuited. Due to the feature of transfer-function zeros locating on the unit circle, we may use an optimization procedure to implement equal-ripple filters. Both low-pass and bandpass filters are realized in the form of microstrip lines and their frequency responses are measured to validate this novel method.**

***Index Terms*—Equal-ripple, microwave filter, nonuniform transmission line, wide-band, Z domain.**

I. Introduction

MICROWAVE filters [1] with their various responses can be manufactured in different forms; examples are low-pass filters with nonuniform transmission lines (NTLs) [2] and bandpass or band-stop filters with coupled lines [3].

Conventional methods to design and implement microwave filters begin with lumped-element prototypes. Lumped-element circuits, with the aid of Richard's transformation [4] and Kuroda's [5] identities, are then transformed to the corresponding distributed-element circuits. Recently, a novel procedure [6] was presented to design and implement microwave filters. It was shown that the transfer function of a network can be formulated in the discrete (or the Z) domain if the network is manufactured by using cascade serial *single* transmission-line sections of the same electrical length.

In this paper, by using the modified transfer functions, discrete filter prototypes, discrete signal-processing techniques [7]–[8], and optimization algorithms, we present a scheme to implement equal-ripple low-pass and bandpass filters over microwave frequencies. We consider networks in which the components are composed of single or *multiple* transmission-line sections of the same electrical length. It can be shown that the chain scattering matrix of each component can be formulated in the discrete domain. As a result, we are able to discuss the chain scattering matrix of the overall network in the Z domain. In particular, we obtain a distinctive property of those shunt components composed of two cascaded transmission-line sections. The transfer function of the network yields conjugate-pair zeros locating on the unit circle if the shunt components are open-circuited. Since two kinds of discrete equal-ripple filters are featured by their transfer functions possessing zeros locating on the unit circle, such a distinctive property of the shunt components is then employed to implement equal-ripple low-pass and bandpass filters over microwave frequencies.

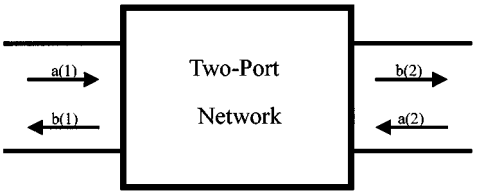

Fig. 1. Two-port network.

Compared with conventional design/implementation methods, the proposed scheme is featured by that it considers the characteristic of equal-delay time of each transmission-line section. As a result, in the Z domain, the scheme finds an *exact* representation for the transfer functions of the networks composed of equal-electrical length transmission-line sections. Since the applied prototypes are also described by functions in the Z domain, we could conclude the characteristics of the prototypes match the nature of the networks used to implement filters. Therefore, prior to the real implementation, a good understanding of the properties of the networks over the frequency bands is obtained. Another distinctive feature of the proposed scheme is that effective components are used to implement zeros locating on the unit circle designated by the transfer functions of the applied prototypes.

To examine the validity of our method, one elliptic low-pass filter and one Chebyshev type-II bandpass filter are manufactured in the form of microstrip lines. The frequency responses of these two filters are measured and elaborated in details in this paper.

II. Transfer Functions in the Discrete Domain

For the block diagram shown in Fig. 1, the chain scattering parameters $T_{mn}, m, n = 1, 2$ of a two-port network are defined by two dependent waves $a(1)$ and $b(1)$ at port 1 and two independent waves $a(2)$ and $b(2)$ at port 2. These waves are interrelated through the chain scattering parameters as follows:

$$\begin{bmatrix} a(1) \\ b(1) \end{bmatrix} = \begin{bmatrix} T_{11} & T_{12} \\ T_{21} & T_{22} \end{bmatrix} \begin{bmatrix} b(2) \\ a(2) \end{bmatrix}. \tag{1}$$

Manuscript received April 10, 2000; revised May 29, 2001. This work was supported by the National Science Council, R.O.C. under Grant NSC 89-2213-E011-137.

The authors are with the Department of Electronic Engineering, National Taiwan University of Science and Technology, Taipei, Taiwan, R.O.C.

Publisher Item Identifier S 0018-9480(02)03013-2.

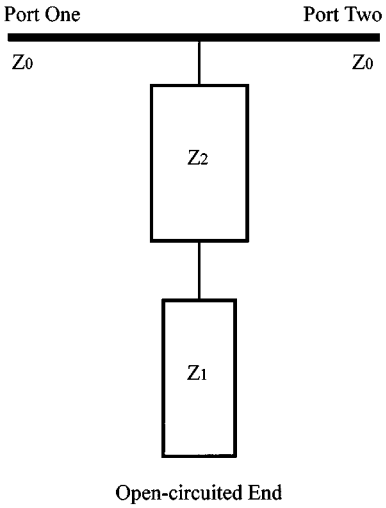

Fig. 2. Open-circuited shunt component composed of two cascaded equal electrical-length transmission-line sections.

Assume that each network consists of serial and shunt components composed of transmission-line sections having length $l = \lambda_0/4$, where λ_0 is the wavelength at the normalizing angular frequency ω_0. In other words, the electrical length of all transmission-line sections is 90° at the frequency ω_0. To convert the frequency-domain behavior into time-domain response, we set $e^{-j2\beta l} = z^{-1}$, where β denotes the propagation constant. It is equivalent to saying that we replace every *double* propagation delay of each transmission-line section by a delay operator. This replacement eventually initiates the elaboration of the design and implementation of microwave filters in the discrete domain.

Fig. 2 shows an open-circuited two-section shunt component. This component is able to contribute zeros locating on the unit circle to the transfer function of the network. The characteristic impedances of the two single-line sections are Z_1 and Z_2. The reflection coefficient γ at the junction of two finite lines is

$$\gamma = \frac{Z_1 - Z_2}{Z_1 + Z_2}. \tag{2}$$

Using the delay operator z^{-1} as the argument, the chain scattering parameters of this shunt component can be expressed as follows:

$$\begin{bmatrix} T_{11} & T_{12} \\ T_{21} & T_{22} \end{bmatrix}_{\text{Two Sec. Shunt}} = \frac{1}{B(z)} \begin{bmatrix} \dfrac{2Z_2B(z) + Z_0A(z)}{2Z_2} & \dfrac{Z_0A(z)}{2Z_2} \\ -\dfrac{Z_0A(z)}{2Z_2} & \dfrac{2Z_2B(z) - Z_0A(z)}{2Z_2} \end{bmatrix} \tag{3}$$

where $B(z) = 1 + 2\gamma z^{-1} + z^{-2}$, $A(z) = 1 - z^{-2}$, and Z_0 is the reference characteristic impedance. The roots of $B(z)$ are $r_1 = -\gamma + \sqrt{\gamma^2 - 1}$ and $r_2 = -\gamma - \sqrt{\gamma^2 - 1}$. Since $|\gamma| \leq 1.0$, both roots r_1 and r_2 are located on the unit circle and they form a conjugate pair.

Two other components are also used to constitute the networks, namely, the short-circuited stub and the serial component having one transmission-line section. The chain scattering parameters associated with the short-circuited stub, as shown in Fig. 3, can be expressed in z^{-1} as follows:

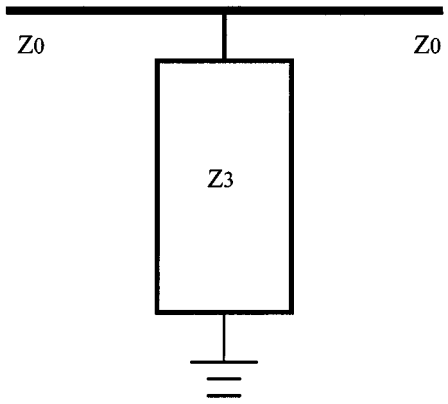

Fig. 3. Short-circuited stub with characteristic impedance Z_3.

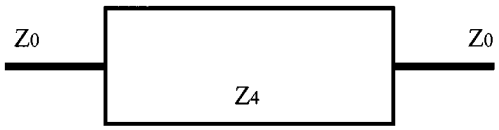

Fig. 4. Serial transmission-line section with characteristic impedance Z_4.

$$\begin{bmatrix} T_{11} & T_{12} \\ T_{21} & T_{22} \end{bmatrix}_{\text{s.c.}} = \frac{1}{1 - z^{-1}} \begin{bmatrix} (1+c) - (1-c)z^{-1} & c + cz^{-1} \\ -c - cz^{-1} & (1-c) - (1+c)z^{-1} \end{bmatrix} \tag{4}$$

where $c = Z_0/(2Z_3)$ and Z_3 is the characteristic impedance of the stub.

On the other hand, the chain scattering parameters of a serial transmission-line section with characteristic impedance Z_4, as illustrated in Fig. 4, can be expressed as follows:

$$\begin{bmatrix} T_{11} & T_{12} \\ T_{21} & T_{22} \end{bmatrix}_{\text{TLS}} = \frac{1}{z^{-1/2}(1 - \Gamma^2)} \begin{bmatrix} 1 - \Gamma^2 z^{-1} & -(\Gamma - \Gamma z^{-1}) \\ \Gamma - \Gamma z^{-1} & -\Gamma^2 + z^{-1} \end{bmatrix} \tag{5}$$

where $\Gamma = (Z_4 - Z_0)/(Z_4 + Z_0)$.

By cascading serial and shunt components orderly to form a network, the overall chain scattering matrix of the network can be found by the sequential multiplication of the chain scattering matrix of each component, i.e.,

$$\begin{bmatrix} T_{11} & T_{12} \\ T_{21} & T_{22} \end{bmatrix}_{\text{Network}} = \prod_{i=1}^{N} \begin{bmatrix} T_{11}^i & T_{12}^i \\ T_{21}^i & T_{22}^i \end{bmatrix} \tag{6}$$

where N is the number of the components used and T_{11}^i, T_{12}^i, T_{21}^i, and T_{22}^i are the matrix elements representing the ith component.

Assume that the network consists of K open-circuited two-section shunt components, L short-circuited stubs, and M serial transmission-line sections. The chain scattering parameter $T_{11}(z)$ of such a network is shown in (7) at the bottom of

this page, where all a_i's are real numbers and are determined by the characteristic impedances of the transmission-line sections composing both serial and shunt components. Note that the polynomial $(1+2\gamma_k z^{-1}+z^{-2})$ comes from the kth open-circuited two-section component $(1-z^{-1})$ comes from each short-circuited stub and $z^{-1/2}\left(1-\Gamma_m^2\right)$ arises from the mth serial transmission line.

If the output port of the network is in a matched termination, the transfer function of the network, denoted as $T(z)$, can be obtained with the inverse of $T_{11}(z)$, i.e.,

$$\begin{aligned} T(z) =& \frac{1}{T_{11}(z)} \\ =& \prod_{m=1}^{M}\left(z^{-1/2}\left(1-\Gamma_m^2\right)\right) \\ & \cdot \frac{\prod_{k=1}^{K}\left(1+2\gamma_k z^{-1}+z^{-2}\right)\prod_{l=1}^{L}\left(1-z^{-1}\right)}{\sum_{i=0}^{2K+L+M} a_i z^{-i}} \\ =& z^{-M/2}\,\frac{\prod_{k=1}^{K}\left(1+2\gamma_k z^{-1}+z^{-2}\right)\prod_{l=1}^{L}\left(1-z^{-1}\right)}{\sum_{i=0}^{2K+L+M} A_i z^{-i}} \end{aligned} \tag{8}$$

where $A_i = a_i/(\prod_{m=1}^{M}\left(1-\Gamma_m^2\right))$, $0 \le i \le 2K+L+M$ are functions of characteristic impedances of transmission lines in either serial or shunt configurations. A close examination on (8) reveals that $T(z)$ has conjugate-pair zeros on the unit circle, which are caused by open-circuited two-section shunt components and zeros at $z=1$, which are due to short-circuited stubs. After these zeros are removed from $T(z)$, the remaining part of the transfer function is recognized as an autoregression (AR) process multiplied by the term $z^{-M/2}$ representing delay factor of the serial components. Denoted as $T_{\mathrm{AR}}(z)$, the AR process is found to be

$$T_{\mathrm{AR}}(z) = \frac{1}{\sum_{i=0}^{2K+L+M} A_i z^{-i}}. \tag{9}$$

Since the AR process is solely characterized by the coefficients A_i and these coefficients can be determined by characteristic impedances of transmission lines, we could make $T_{\mathrm{AR}}(z)$ approximate a proposed AR process by adjusting the values of the impedances.

III. Realization of Filters

In this section, we present the procedure to realize both low-pass equal-ripple filters and bandpass equal-ripple filters. The procedure is briefly described as follows.

1) Propose a digital filter prototype $F(z)$, which satisfies the required specifications. Besides, refer to the zero locations of $F(z)$, and then determine the configuration of the network that attempts to synthesize the filter.
2) Find $T(z)$ by (8), where the numerator of $T(z)$ could be determined explicitly according to the configuration of the network. Divide both $T(z)$ and $F(z)$ by the numerator of $T(z)$ that generates zeros on the unit circle. The function derived from $F(z)$ is denoted as $\bar{F}(z)$.
3) Find an equivalent AR process of $\bar{F}(z)$, denoted as $F_{\mathrm{AR}}(z)$ and cast it in the following form:

$$F_{\mathrm{AR}}(z) = \frac{1}{\sum_{i=0}^{2K+L+M} A_i' z^{-i}} \tag{10}$$

where, as stated in the previous section, K, L, and M are numbers of three kinds of components employed to synthesize the filter.
4) Adjust the values of characteristic impedances of all transmission lines with optimization algorithms so that A_i in (9) and A_i' in (10) are as close as possible in the least square error (LSE) sense.

Another important design criterion is that the open-circuited two-section shunt components are obtained according to the real parts of conjugate-pair zeros locating on the unit circle of the proposed prototype $F(z)$. In other words, if the real part of one pair of the conjugate zeros is α, the γ in (2) associated with one open-circuited two-section shunt component is set to be $\gamma = -\alpha$. Thus, when the value of Z_2 that composes this kind of component is determined, the value of another impedance, i.e., Z_1, can be found from (2).

A. Implementation of Low-Pass Filters

To realize filters, the reference characteristic impedance Z_0 is always set to be 50 Ω. Considering the realization of a low-pass filter with its cutoff frequency equal to 1.2 GHz, we adopt a prototype $F(z)$ as follows:

$$F(z) = \frac{\sum_{j=0}^{4} b_j z^{-j}}{\sum_{i=0}^{4} a_i z^{-i}} \tag{11}$$

where

$$\{b_j, 0 \le j \le 4\} = \{0.0353,\ 0.0234,\ 0.0561,\ 0.0234,\ 0.0353\}$$

and

$$\begin{aligned} &\{a_i, 0 \le i \le 4\} \\ &\qquad = \{1.0000, -2.3210,\ 2.6772, -1.5774,\ 0.4158\}. \end{aligned}$$

$$T_{11}(z) = \frac{\sum_{i=0}^{2K+L+M} a_i z^{-i}}{\prod_{k=1}^{K}\left(1+2\gamma_k z^{-1}+z^{-2}\right)\prod_{l=1}^{L}\left(1-z^{-1}\right)\prod_{m=1}^{M}\left(z^{-1/2}\left(1-\Gamma_m^2\right)\right)} \tag{7}$$

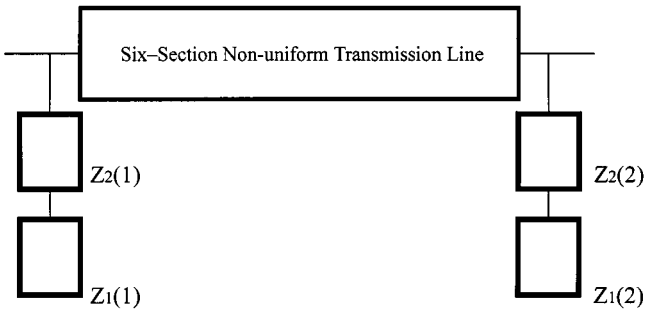

Fig. 5. Configuration of the elliptic low-pass filter.

This prototype describes an elliptic low-pass filter, of which the ripple over the passband is 1 dB and the ripple over the stopband is 40 dB. As the cutoff frequency of this prototype is equal to $0.3\omega_0$, the normalizing angular frequency should be $\omega_0 = 2\pi \times (4 \times 10^9)$ rad/s so that the prototype meets the specification at the cutoff frequency. Note that four roots of the numerator of $F(z)$ form two pairs of conjugate-pair zeros located on the unit circle and the real parts of zeros are -0.5267 and 0.1958.

The configuration of transmission-line circuit attempting to synthesize the proposed low-pass filter is shown in Fig. 5. There are two open-circuited two-section shunt components: one, composed of $Z_1(1)$ and $Z_2(1)$, is at port 1 and the other, composed of $Z_1(2)$ and $Z_2(2)$, is at port 2; between these two shunt components, there is a six-section NTL. Since two shunt components are designed according to real parts of the conjugate-pair zeros of $F(z)$, the transfer function of the network $T(z)$ in (8), has the same zeros as those of $F(z)$. In addition, we know that the order of the denominator of $T(z)$ is ten since, for this network, we have $K = 2$, $L = 0$, and $M = 6$. Due to the cancellation of zeros of $F(z)$ by those of $T(z)$, the coefficients A_i' associated with the function $F_{\mathrm{AR}}(z)$ in (10) can be found directly by the denominator of $F(z)$, namely, $A_i' = a_i/b_0$ for $0 \le i \le 4$ and $A_i' = .0$ for $5 \le i \le 10$.

Let the values of A_i' be the ideal values of the coefficients A_i in (9). We use optimization algorithms to adjust $Z_2(1)$, $Z_2(2)$, and the characteristic impedances of the transmission lines composing the NTL such that the value of $\sum_{i=0}^{10}(A_i - A_i')^2$ is minimized. The optimal values for $Z_2(1)$ and $Z_2(2)$ are 80.3 and 103.2 Ω, respectively. The values of $Z_1(1)$ and $Z_1(2)$, which form the other part of two open-circuited two-section shunt components, are $Z_1(1) = 259.0\ \Omega$ and $Z_1(2) = 69.4\ \Omega$. The values for the characteristic impedances of six transmission-line sections, from the left- to right-hand side, are 143.8, 11.6, 160, 14.8, 148.1, and 99.4 Ω. Both the magnitude responses of $T(z)$ and $F(z)$ are presented in Fig. 6. We could see that there exists a good agreement between these two functions.

To validate the effectiveness of our method, the optimal values obtained by optimization algorithms are used to manufactured the network in the form of microstrip lines. However, due to the limitation caused by the available manufacturing technique, the largest value of all characteristic impedances is limited to be 160 Ω. Therefore, the characteristic impedances of the first shunt component should be modified to meet this constrain; the values of $Z_1(1)$ is set to be 160.0 Ω and, while maintaining the value of the associated γ unchanged, the new

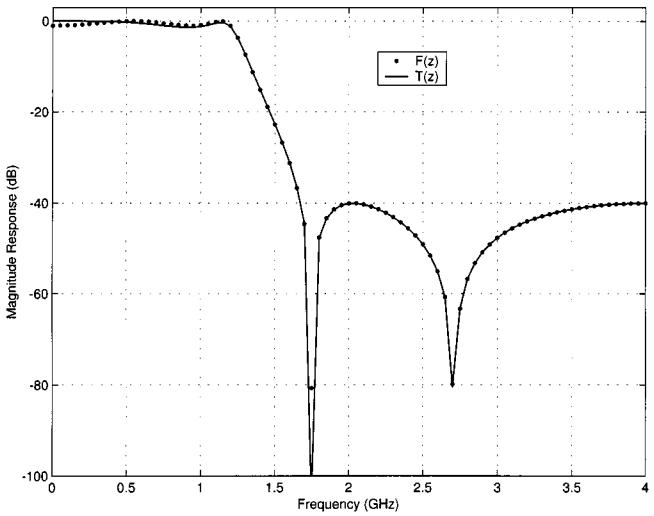

Fig. 6. Magnitude responses of both $F(z)$ and $T(z)$ for the low-pass filter with its cutoff frequency equal to 1.2 GHz.

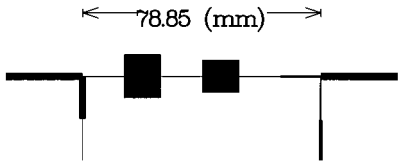

Fig. 7. Layout of the low-pass filter in the form of microstrip lines.

values of $Z_2(1)\ \Omega$ is 49.6 Ω. The layout of the filter is presented in Fig. 7, where the substrate used is Duroid, of which the relative dielectric constant is 2.5 and the height is 0.787 (mm) or 1.0 (mil). The left-hand side of the network is port 1 and the right-hand side is port 2. On both sides, the reference impedance lines (50 Ω) are placed and all finite transmission lines have electrical length of 90° at 4.0 GHz. As illustrated, the total length of the filter is 78.85 (mm).

We use an HP 8510C network analyzer to measure both reflected and transferred parameters, i.e., S_{11} and S_{21}. The magnitude responses of the two measured parameters are presented in Fig. 8. In this figure, to facilitate the comparison between design data and measurement results, magnitude response of the ideal S_{21} is also plotted. The ripple of measured S_{21} over the passband is less than 1.0 dB, as required by $F(z)$ in (11); the ripple of the measured S_{21} over the stopband deviates from the ideal value 40 dB because of the modification of $Z_1(1)$ and $Z_2(1)$. The zeros of measured S_{21} occur at 1.72 and 2.67 GHz. These values are very close to the zeros of $F(z)$, which are 1.75 and 2.7 GHz.

Besides, comparing the measured S_{21} with the ideal S_{21}, we find that the insertion-loss rate of measured S_{21} over the stopband is in good agreement with that of the ideal S_{21}. However, because of the effect of discontinuities of steps, T-junctions and open-circuited ends of the components, the passband bandwidth of measured S_{21} (1.1 GHz) is smaller than that of the ideal S_{21} (1.2 GHz).

B. Realization of Bandpass Filters

A Chebyshev type-II bandpass filter is discussed in this section. The ripple of the stopband is 40 dB. In addition, the band-

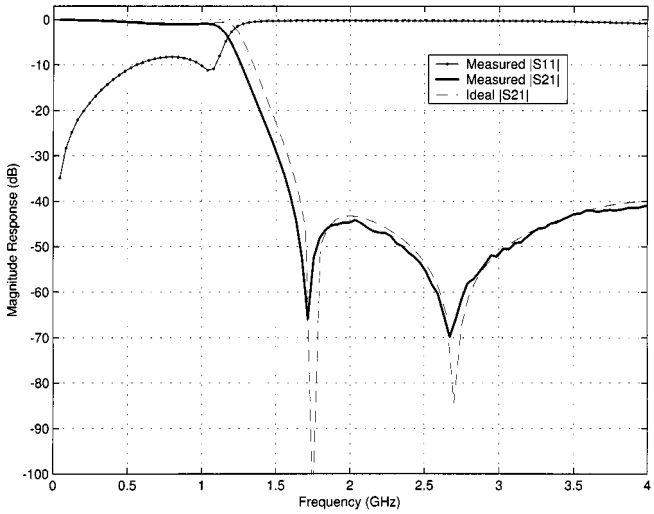

Fig. 8. Measured reflected and transferred scattering coefficients at input and output ports of the low-pass filter shown in Fig. 7.

width is set to be 80% and the central frequency is 4.0 GHz. Therefore, the normalizing angular frequency ω_0 is equal to $2\pi \times (4 \times 10^9)$ rad/s. The prototype satisfying the specification is as follows:

$$F(z) = \frac{\sum_{j=0}^{5} b_j z^{-j}}{\sum_{i=0}^{5} a_i z^{-i}} \tag{12}$$

where

$$\{b_j, 0 \le j \le 5\} = \{0.0317, -0.0283, 0.0530, -0.0530, 0.0283, -0.0317\}$$

and

$$\{a_i, 0 \le i \le 5\} = \{1.0000, 2.0909, 2.2195, 1.2356, 0.3793, 0.0465\}.$$

There are five zeros in $F(z)$: one is at $z = 1$ and the other four form two pairs of conjugate-pair zeros locating on the unit circle, of which the real parts are -0.2630 and 0.2088.

The configuration of the network to synthesize the bandpass filter is shown in Fig. 9. There are two open-circuited two-section shunt components: one, composed of $Z_1(1)$ and $Z_2(1)$, is at port 1 and the other, composed of $Z_1(2)$ and $Z_2(2)$, is at port 2. Both of two shunt components are designed according to the real parts of the conjugate-pair zeros of $F(z)$ shown in (12). Between two shunt components, the circuit can be divided into two parts; one part comprises four transmission-line sections interlaced with four short-circuited stubs and the other is a six-section NTL.

With $F_{\mathrm{AR}}(z)$ associated with $F(z)$ in (12) and $T_{\mathrm{AR}}(z)$ associated with $T(z)$ in (8), the optimization algorithms give the optimal values of transmission-line characteristic impedances. The impedance values for two open-circuited shunt components are $Z_2(1) = 112.7\ \Omega$, $Z_2(2) = 160.0\ \Omega$, $Z_1(1) = 193.1\ \Omega$, and $Z_1(2) = 104.7\ \Omega$. In addition, from the left- to right-hand side in Fig. 9, the four serial transmission-line sections are 49.6, 74.0, 127.6, and 160.0 Ω; the four short-circuited stubs are 21.1, 36.7, 71.5, and 160.0 Ω; and the six characteristic impedances of NTL are 108.4, 39.1, 21.1, 35.8, 72.7, and 64.3 Ω. Fig. 10 shows the numerical values of both $F(z)$ and $T(z)$. The results show that the response of $T(z)$ is in good agreement with that of $F(z)$.

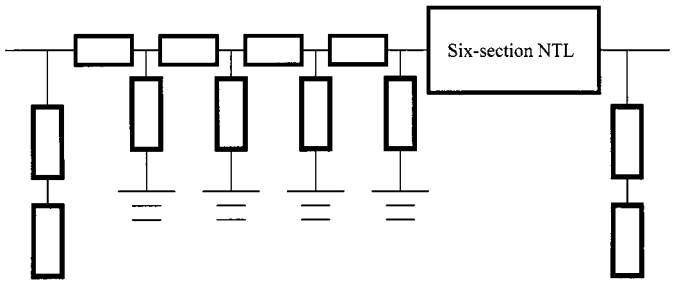

Fig. 9. Configuration of the Chebyshev type-II bandpass filter.

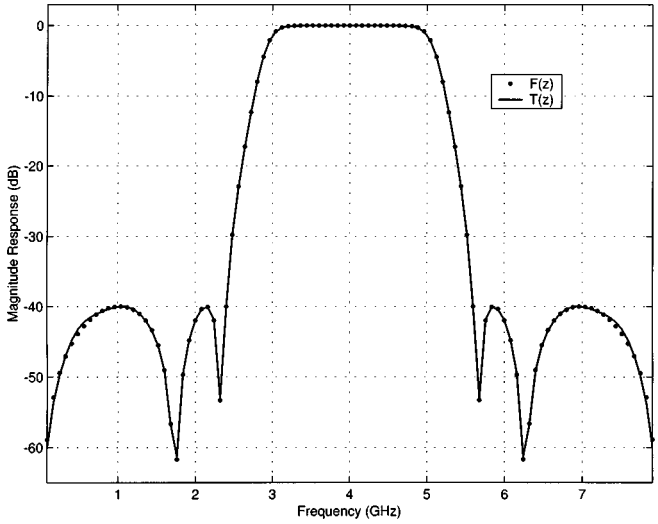

Fig. 10. Magnitude responses of both $F(z)$ and $T(z)$ for the bandpass filter with central frequency at 4.0 GHz and bandwidth of 80%.

The network is fabricated on the same Duroid substrate mentioned in Section III-A. Again, the value of $Z_1(1)$ should be modified to 160 Ω so that its value could meet the constraint caused the available manufacturing technique. As a result, $Z_2(1)$ should be changed accordingly. The new value of $Z_2(1)$ is 94.3 Ω. The layout of the bandpass filter is shown in Fig. 11, where the total length of the filter is 131.064 mm. Fig. 12 shows the magnitude responses of measured scattering parameters S_{11} and S_{21} of this filter. To facilitate the comparison between design data and measurement results, the magnitude response of the ideal S_{21} is also presented in Fig. 12. The zeros of measured S_{21} occur at 1.68, 2.3, 5.63, and 6.18 GHz, being very close to the zeros of $F(z)$, which are 1.78, 2.28, 5.73, and 6.23 GHz. Due to loss factors of the substrate and conductor, the magnitude of measured S_{21} over the passband is approximately -0.6 dB compared to the ideal value 0 dB. In addition, because of the modification of $Z_1(1)$ and $Z_2(1)$, the ripple of S_{21} over the stopband region deviates from the ideal values of 40 dB.

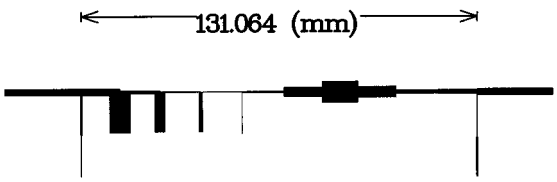

Fig. 11. Layout of the bandpass filter in the form of microstrip lines; note that each single-section shunt stub is short-circuited by multiple via-holes along the edge.

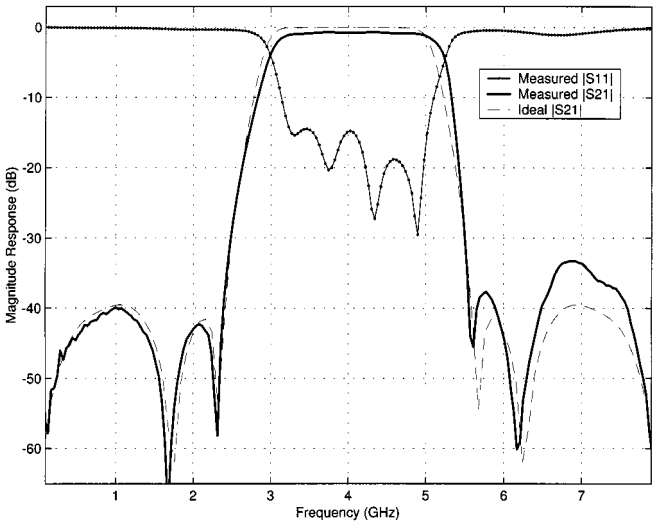

Fig. 12. Measured reflected and transferred scattering coefficients at input and output ports of the bandpass filter shown in Fig. 11.

Besides, comparing the measured S_{21} with the ideal S_{21}, we find that the insertion-loss rate of the measured S_{21} is approximately the same as that of the ideal S_{21} over the stopbands. However, because of the nonideal discontinuities of steps, junctions, and ends of the components, the central frequency of the measured S_{21} moves to 4.1 GHz. The effects of the discontinuities could also account for the less attenuation of the measured S_{21} than that of the ideal S_{21} over the higher stopband.

IV. Conclusion

An effective approach to realize equal-ripple low-pass and bandpass filters over microwave frequencies has been presented in this paper. Since the mathematical formulation of filters is expressed in terms of discrete-time signal processing, this scheme is suitable for computer-aided design (CAD) engineering applications. The theoretical values are verified with practical implementations where circuits are realized with microstrip transmission lines. The experimental results are in good agreement with theoretical values, which illustrates the validity of the proposed approach and circuit configuration.

Finally, we make a remark about the optimization method. When characteristic impedances obtained are larger than the limit of the available manufacturing technique, one may use more components to implement the networks. For example, when the optimization method could not find a suitable solution to the impedances of a network with a certain configuration, one could use more serial transmission-line sections to implement the networks to increase the opportunity of finding a suitable solution or one could use two open-circuited two-section components to implement one zero locating on the unit circle.

References

[1] G. L. Matthaei, L. Young, and E. M. T. Jones, *Microwave Filters, Impedance-Matching Networks and Coupling Structures*. Norwood, MA: Artech House, 1980.

[2] M. L. Roy, A. Pérennec, S. Toutain, and L. C. Calvez, "The continuously varying transmission-line technique-application to filter design," *IEEE Trans. Microwave Theory Tech.*, vol. 47, pp. 1680–1687, Sept. 1999.

[3] S. B. Cohn, "Parallel-coupled transmission-line-resonator filters," *IRE Trans. Microwave Theory Tech.*, vol. MTT-6, pp. 223–231, Apr. 1958.

[4] P. I. Richard, "Resistor-transmission line circuits," *Proc. IRE*, vol. 36, pp. 217–220, Feb. 1948.

[5] K. Kuroda, "General properties and synthesis of transmission-line networks," in *Microwave Filters and Circuits*, A. Matsumoto, Ed. New York: Academic, 1970, vol. 22.

[6] T. W. Pan and C. W. Hsue, "Modified transmission and reflection coefficients of nonuniform transmission lines and their applications," *IEEE Trans. Microwave Theory Tech.*, vol. 46, pp. 2092–2097, Dec. 1998.

[7] A. V. Oppenheim and R. W. Schafer, *Discrete-Time Signal Processing*. Englewood Cliffs, NJ: Prentice-Hall, 1989.

[8] S. Haykin, *Adaptive Filter Theory*. Englewood Cliffs, NJ: Prentice-Hall, 1996.

Da-Chiang Chang was born in Taipei, Taiwan, R.O.C., in 1966. He received the B.S. and M.S. degrees in electrical engineering from the National Tsing-Hua University, Hsin-Chu, Taiwan, R.O.C., in 1989 and 1991, respectively, and is currently working toward the Ph.D. degree in electronic engineering at the National Taiwan University of Science and Technology, Taipei, Taiwan, R.O.C.

From July 1991 to June 1993, he was an officer in the R.O.C. Air Force. In Fall 1993, he joined the Department of Electronic Engineering, Chinese Institute of Technology, Taipei, China, where he is currently an Instructor. His current interests are in discrete-time signal processing, wireless communications, and RF and analog circuit design.

Chin-Wen Hsue (S'85–M'85–SM'91) was born in Tainan, Taiwan, R.O.C. He received the B.S. and M.S. degrees in electrophysics and electronic from the National Chiao-Tung University, Hsin-Chu, Taiwan, R.O.C., in 1973 and 1975, respectively, and the Ph.D. degree from the Polytechnic University (formerly the Polytechnic Institute of Brooklyn), Brooklyn, NY, in 1985.

From 1975 to 1980, he was a Research Engineer at the Telecommunication Laboratories, Ministry of Communication, Taiwan, R.O.C. From 1985 to 1993, he was with Bell Laboratories, Princeton, NJ, as a Member of Technical Staff. In 1993, he joined the Department of Electronic Engineering, National Taiwan University of Science and Technology, Taipei, Taiwan, R.O.C., as a Professor, and from August 1997 to July 1999, he was the Department Chairman. His current interests are in pulse-signal propagation in lossless and lossy transmission media, wave interactions between nonlinear elements and transmission lines, photonics, high-power amplifiers, and electromagnetic inverse scattering.